Segmentation of Multiple Sclerosis Lesions in MRI-An Image Analysis Approach

K. Krishnan and M. S. Atkins

Department of Computer Science.
Simon Fraser University, Burnaby, B.C., Canada.

ABSTRACT

This paper describes an intensity-based method for the segmentation of multiple sclerosis lesions in dual-echo PD and T2-weighted magnetic resonance brain images. The method consists of two stages: feature extraction and image analysis. For feature extraction, we use a ratio filter transformation on the proton density (PD) and spin-spin (T2) data sequences to extract the white matter, cerebrospinal fluid and the lesion features. The one and two dimensional histograms of the features are then analysed to obtain different parameters, which provide the basis for subsequent image analysis operations to detect the multiple sclerosis lesions. In the image analysis stage, the PD images of the volume are first pre-processed to enhance the lesion tissue areas. White matter and cerebrospinal fluid masks are then generated and applied on the enhanced volume to remove non-lesion areas. Segmentation of lesions is performed in two steps: conspicuous lesions are extracted in the first step, followed by the ext raction of the subtle lesions.

The method was tested on the data from eight patients with total manual lesion volumes ranging from 200 to 28000 mm^3 Each data set had dual echo PD and T2 images. The manual segmentation of the data was done independently by a trained technologist. The automatic segmentation results were analysed by comparisons with the manual segmentation of the same scans, using similarity index and total lesion volume correlation figures. Results show a total volume correlation of 0.972.

Keywords: Segmentation, Feature extraction, Image analysis

1. INTRODUCTION

Segmentation of Magnetic Resonance (MR) images has many applications as a diagnostic tool because it provides a basis to extract useful measurements or information from the MR image fields. One major use of MR images is for quantitation of Multiple Sclerosis (MS) lesions. Despite extensive research in this area, there still exists a need for the development of automatic image analysis techniques to segment and quantify MS lesions. The MRI data is characterised by its multispectral nature. Each pixel from an MR image represents many tissue parameters, typically, proton density (PD), spin-lattice (T1) and spin-spin (T2) relaxation time. Many of the current segmentation algorithms exploit the multispectral nature of MRI for 2D and 3D segmentation and classification [1], [2], [3], [4]. Although the multispectral nature of MRI provides more information for improved segmentation performance, the vast amount of data that is generated and the intensity variations due to RF inhomogenities, motion artifacts and noise, render the problem of segmentation difficult.

In our work, we have adopted the notion of feature extraction for multispectral MRI segmentation [5]. In feature extraction, a measurement pattern or vector is processed to extract the features relevant to the problem under study, which in our case is the problem of detecting the MS lesions. Our efforts focus on using multispectral techniques of image analysis for segmentation with the aim of realizing two major goals: to obtain a reliable and consistent segmentation performance for the whole volume of data, and to minimize the human intervention. In this paper, we propose a method that is based on various features resulting from a novel ratio filter transformation of the PD and T2 data sequences.

Details of the methodology are presented in Section 2. A single slice from a particular data set has been chosen to illustrate the results from various stages of processing. Results on the segmentation performance on the whole volume of 8 data sets is discussed in Section 3. Conclusions are derived in Section 4.

Part of the SPIE Conference on Image Processing • San Diego, California • February 1998
SPIE Vol. 3338 • 0277-786X/98/$10.00

2. METHOD

Overview

Figure 1 illustrates our method for MS lesion segmentation. The system consists of two main stages: feature extraction and image analysis. In the feature extraction stage, the spatial pixel intensities of the PD and T2 volume are transformed using a ratio filter and thresholded at different levels to obtain an initial segmentation of the tissues of interest: here we extract the white matter (wm) and the cerebrospinal fluid (csf). An analysis of the one and two dimensional histograms of the segmented tissues provide the necessary thresholding parameters for subsequent image analysis operations. The details are presented in Section 2. 2.

In the image analysis stage, the PD and T2 volumes are processed to detect the MS lesions, using the features and parameters from the initial stage. The image analysis is carried out in two steps: first, extraction of the conspicuous lesions, which are then used to extract conspicuous and subtle lesions. For each step, the lesion tissue areas are enhanced in the PD volume and then identified using wm and csf masks. The procedure is explained in detail in Section 2.3.

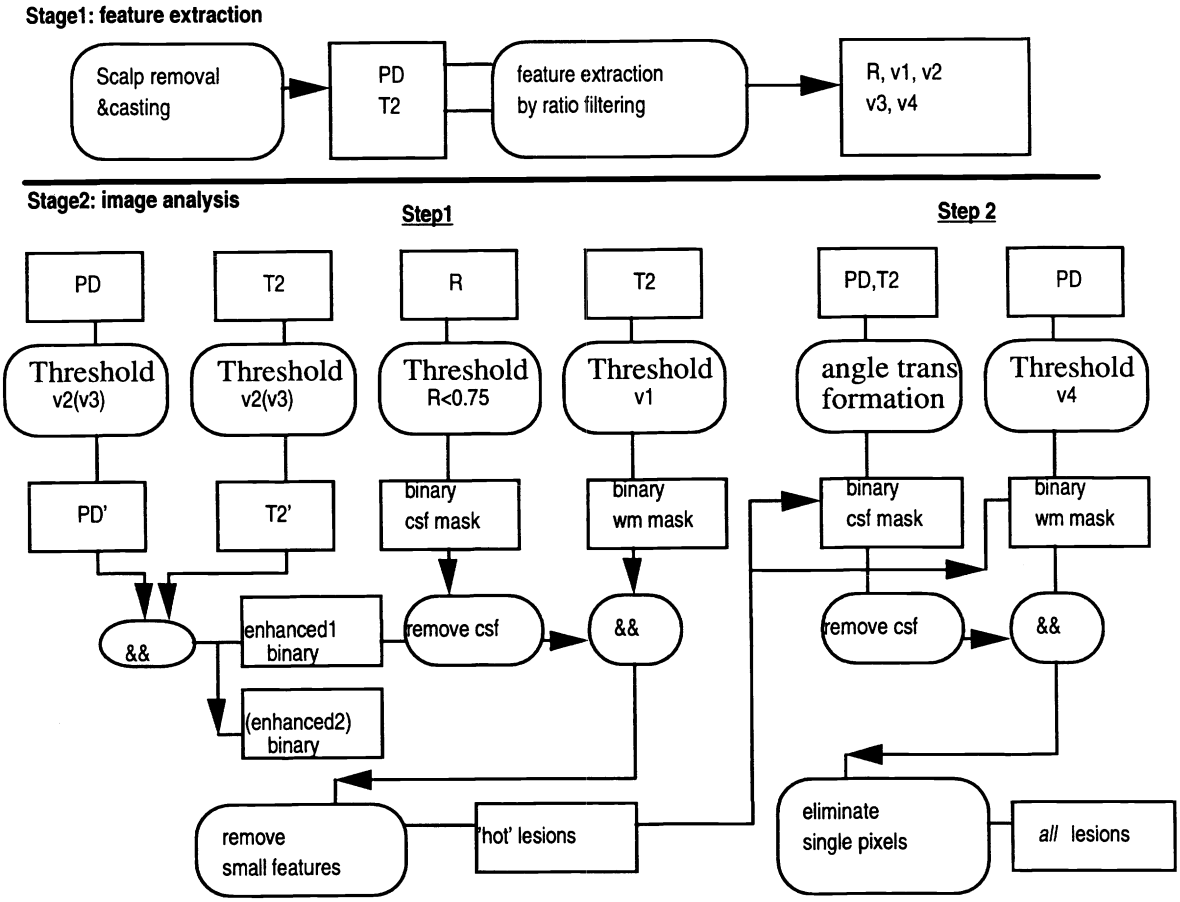

Figure 1: System overview

Stage1: Feature Extraction

The data consists of a dual echo MRI sequence PD-weighted (TE = 30ms) and T2-weighted (TE = 90ms, TR = 2.5secs), each image consisting of 24 slices of dimension 256x256. The data was acquired in the axial plane on a General Electric 1.5 Tesla MRI scanner. Each voxel measures 0.859 x 0.859 x 5.0 mm in the x, y and z planes

respectively with a slice gap of 0.5mm. The acquired images are converted from the original 12 bit to 8 bit by casting the volume data around the mean . The non-brain tissues like meninges, skin, fat and bone are masked out using an automatic masking algorithm [6]. The masking operation need not be perfect because our subsequent processing easily removes extraneous tissues. Next, the brain data is transformed using a ratio filter [7], [8]. In our studies, we use the filter on the PD and T2 image planes using a simple relation

$$R(i,j) = \left[\frac{PD\ (i,j)}{T2\ (i,j)}\right]$$

on each pixel. where PD(i,j) and T2(i,j) are the pixel intensities at the spatial location (i,j) for PD and T2 respectively. By taking the ratio of the images, most of the signal variations within a specific tissue are compensated, thereby improving the signal to noise ratio [8]. An example of the ratio image is shown in Figure 2(c), with Figure 2(a) and 2(b) showing the original PD and T2 slices.

The stage-1 feature extraction is done by thresholding the ratio image to obtain a new image R', and generating a feature mask, based on the pixels in the PD image that contribute to R'. Different thresholds are used to create a different R' for each tissue type. This stage currently requires manual thresholding, although in future, we believe it can be automated to obtain the threshold parameters as the feature plots of the ratio image show good separation of csf and lesions. The ratio image and the feature masks resulting from the thresholding process are shown in Figure 2(c)-(f). The same threshold parameters are used on all the slices of the ratio image volume; there is no need to compensate for RF inhomogeneity along the axis.

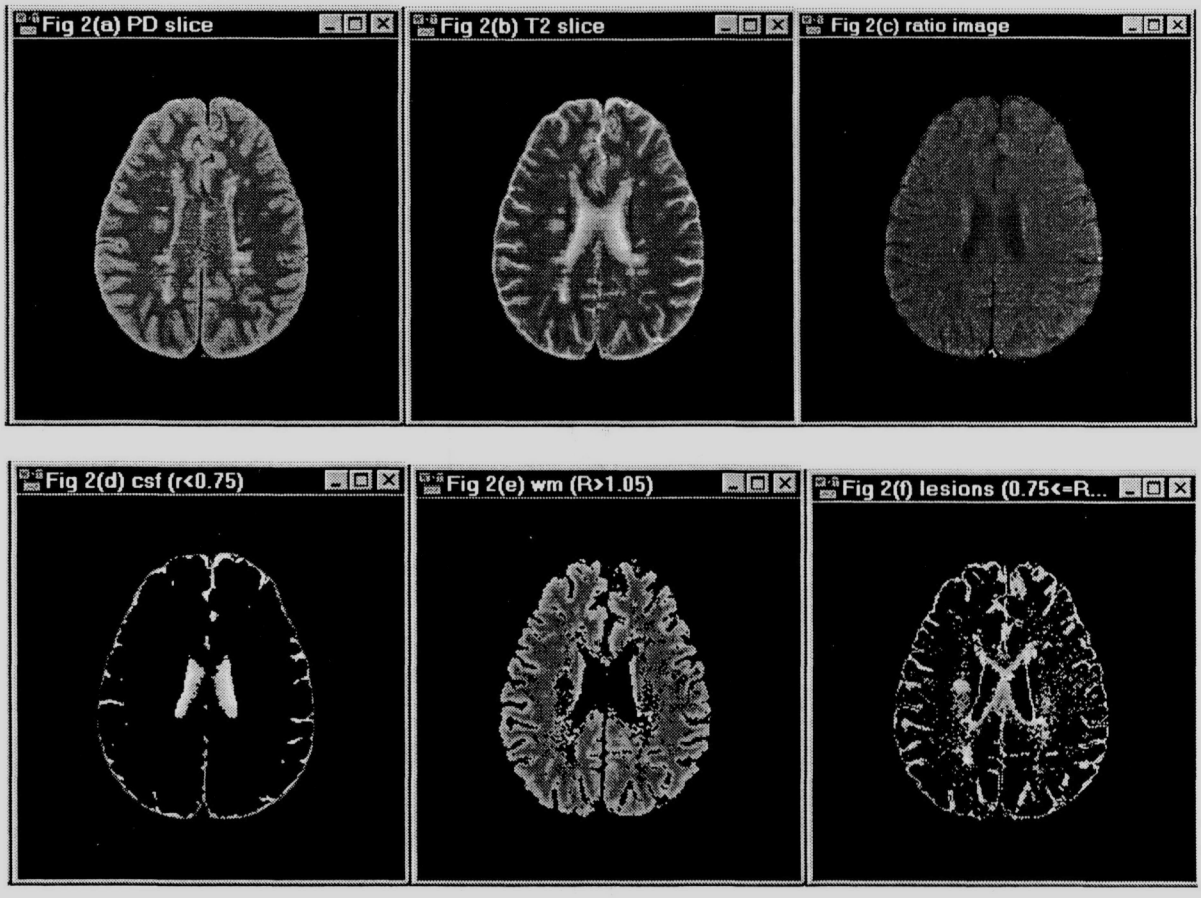

Figure 2: Gray scale feature masks from stage-1 processing for a single slice .
(a) and (b) original PD and T2 slice 15 (c) ratio image (PD-intensity/T2-intensity) (d)-(f) csf, wm and lesion masks

The 1-D histogram of a slice from the T2 and PD images *before* stage-1 processing is shown in Figure 3(a) and (b). The tissue profiles of the features obtained above *after* stage-1 processing are shown by the 1-D histograms in Figure 3(c) and (d).

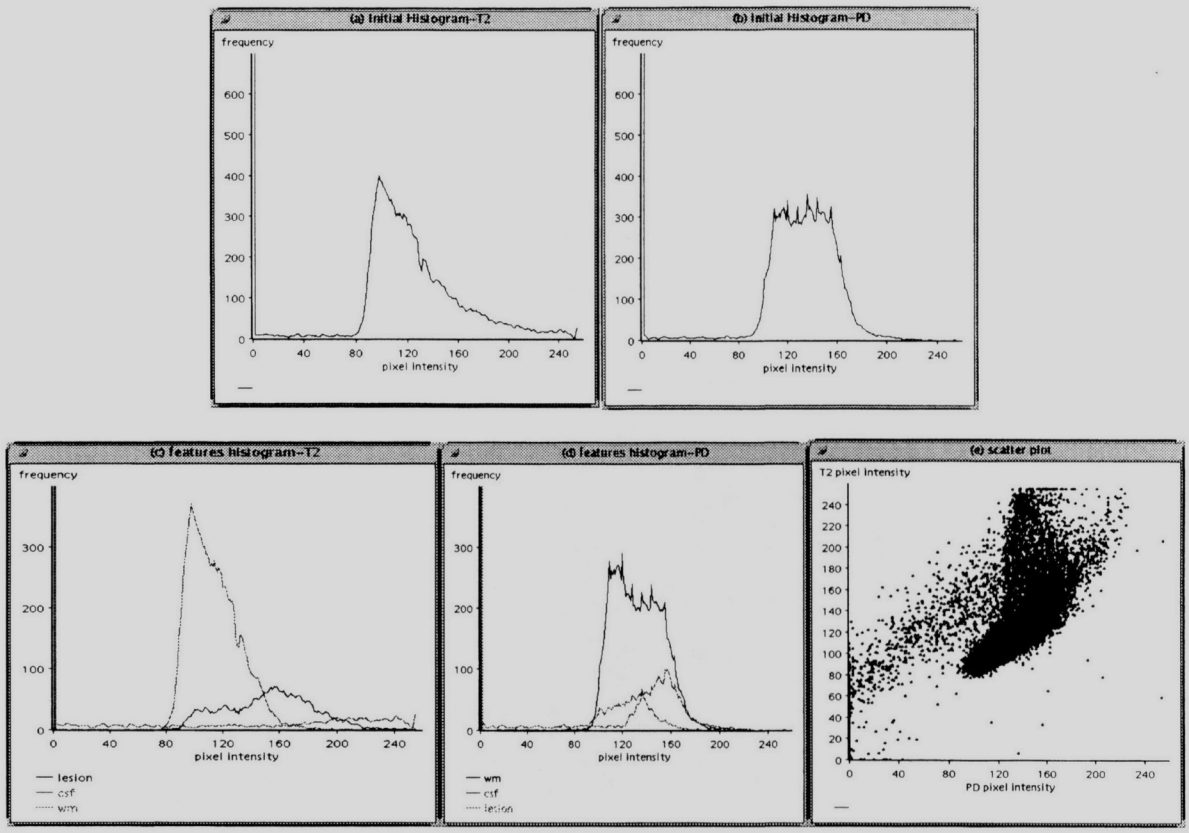

Figure 3: 1 and 2-dimensional histograms of the feature masks of stage-1 for slice 15. 3 (a), (b) initial histograms for T2 and PD. (c), (d) histogram profile of the feature masks. (e) scatter plot of PD and T2

Observe that the wm tissue histogram is seen well separated from the other tissue histograms, at least, from the high intensity lesions and the csf in the T2 image as a result of stage-1 operations explained above. This suggests that the wm areas can be easily extracted using a simple thresholding operation on the T2 volume. The histogram for PD shows how difficult it would be to segment from the PD alone. We observed a similar pattern of histogram profiles for other slices in the volume (it should be noted that the histograms shown correspond to the data set used in our study with the echo sequence mentioned earlier). The 2-D histogram of the same slice is shown as a scatter plot in Figure 3(e).

From the analysis of 1 and 2-D histograms for the whole volume, we obtain four parameters v1 (80,145), v2 (165, 255), v3 (145, 255) and v4(80, 132) for thresholding; these parameters are used in the stage 2 analysis detailed below. The parameter v1 is used on T2 for wm thresholding. The parameter v2 is used on PD to enhance high intensity lesion and is obtained from the 2-D histogram. Parameter v3 is used on PD to enhance *all* the lesions of the volume. v4 is used on PD for wm thresholding. The same parameters are used on all slices of the volume.

Stage 2: Image analysis system.

Step1: First, we process the PD images of the volume to enhance the areas of conspicuous lesions. Conspicuous lesions are identified as blob features with high intensity profiles in both PD and T2 images and a minimum size of 3 pixels width and height. It is necessary to identify the conspicuous lesions because they otherwise appear as false positives in generating the csf mask thereby affecting the final results of segmentation.

To enhance the areas of conspi cuous lesions, the PD image is first thresholded with the value v2 to form a gray scale image PD'. Thresholding by v2 highlights the high intensity areas in the PD and T2 images, and is shown in Figure 4(a) and 4(b) for the selected slice. Then a new image (PD' && T2') which we call PD" is obtained to extract the areas that appear as " **hot**" lesions in both PD and T2. The resulting enhanced, binary image called "enhanced1 mask" is shown in Figure 4(c), which includes " **hot**" lesions and other high intensity pixels that arise from flow artifacts. To remove many of these non-lesion areas, we threshold the T2 image with v1, as shown in Figure 4(d) which leaves mostly wm and apply the mask to the enhanced image . This "cleans up" the hot lesion volume, especially for the lower brain slices in the volume. Finally, a csf mask is made from the csf feature image (obtained from thresholding the ratio image as shown in Figure 2(d)). The mask has a value set ON, whenever the ratio image >0, and is shown in Figure 4(e). The mask is applied to PD" to remove spurious false hot spots arising in the image. The features with size of 3 pixels are identified as conspicuous lesions in the resulting image. The conspicuous lesions are shown in Figure 4(f).

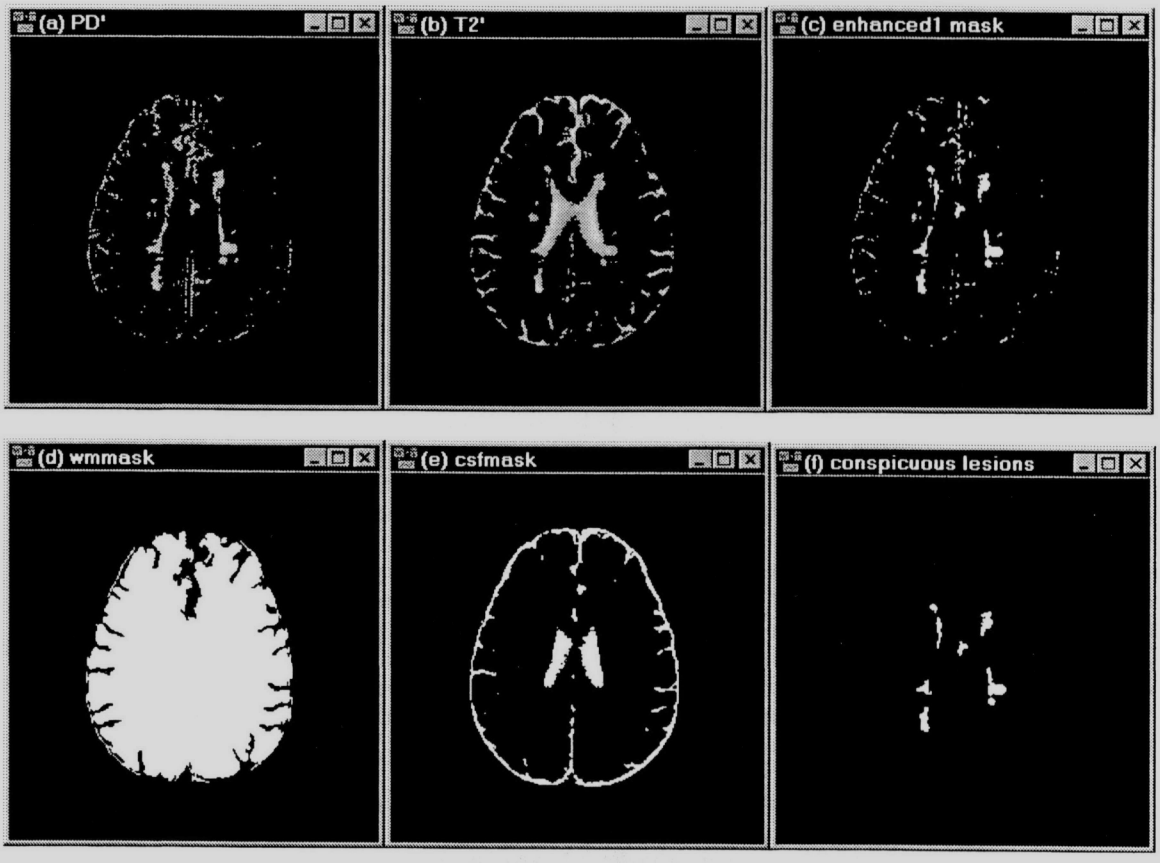

Figure 4: Stage-2 processing results for detection of cons picuous lesions on slice 15. (a) PD' (b) T2' (c) slice 15 after enhancement (d) wm (e) csf and (f) the conspicuous lesions on slice 15.

Step2: To extract the conspicuous *and* subtle lesions, the enhanced image "enhanced2 mask" shown in Figure 5 c is obtained as explained above, but using the threshold value v3 on PD so as to include *all* the lesions, as shown in Figure 5(a). To obtain the images shown in Figure 5(b) - 5(e), we have followed the same operations explained under Step1. The wm mask shown in Figure 5(d) is obtained by thresholding the PD image with the value v4. The false negative lesions in the wm mask are removed using the conspicuous lesions, obtained in Step1. As can be seen from the enhanced image in Figure 5(c), the detection of subtle lesions requires a more precise csf mask to extract periventricular lesions carefully from the csf. To extract the csf feature, we use the angle transformation approach explained in [3]. The resulting angle image is thresholded to generate the csf mask, shown in Figure 5(e). The false positive lesions in the csf mask are removed using the conspicuous lesions, obtained in step1. The extracted lesions are shown in Figure 5(f).

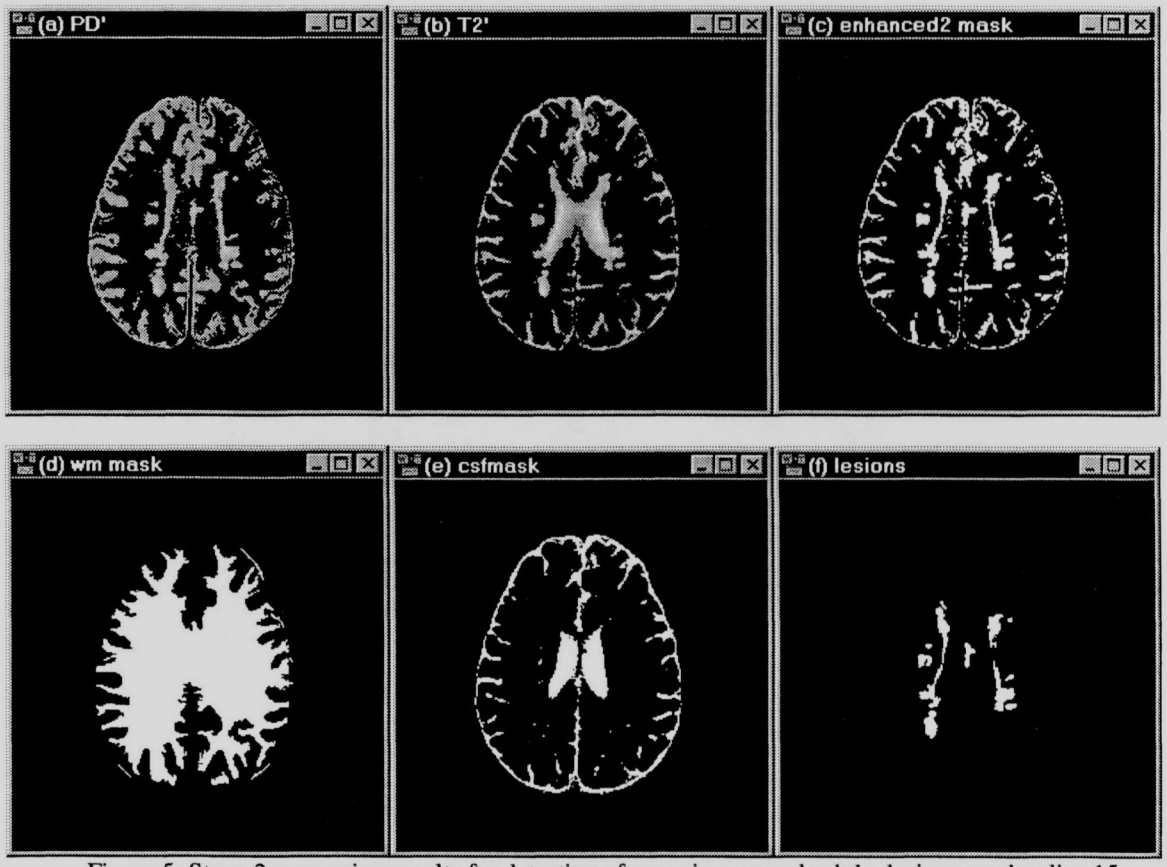

Figure 5: Stage-2 processing results for detection of conspicuous and subtle lesions on the slice 15 PD' (b) T2' (c) slice 15 after enhancement (d) wm (e) csf and (f) the segmented lesions on the slice 15.

3. RESULTS

The method was tested on the whole volume of 8 different sets of data. Figure 6 shows the lesions manually outlined by a trained technician on the PD scan of a specific data set on the central slices of the volume, after casting and masking out for non-brain tissues. For visual comparison, Figure 7 shows the lesions found automatically by our method. Note that the bright patches on the right hand side of the last two slices have correctly not been found to be a lesion; nor have the bright areas near the centre been falsely identified as lesions. It should also be noted that the method has not identified all th e subtle lesions in the volume.

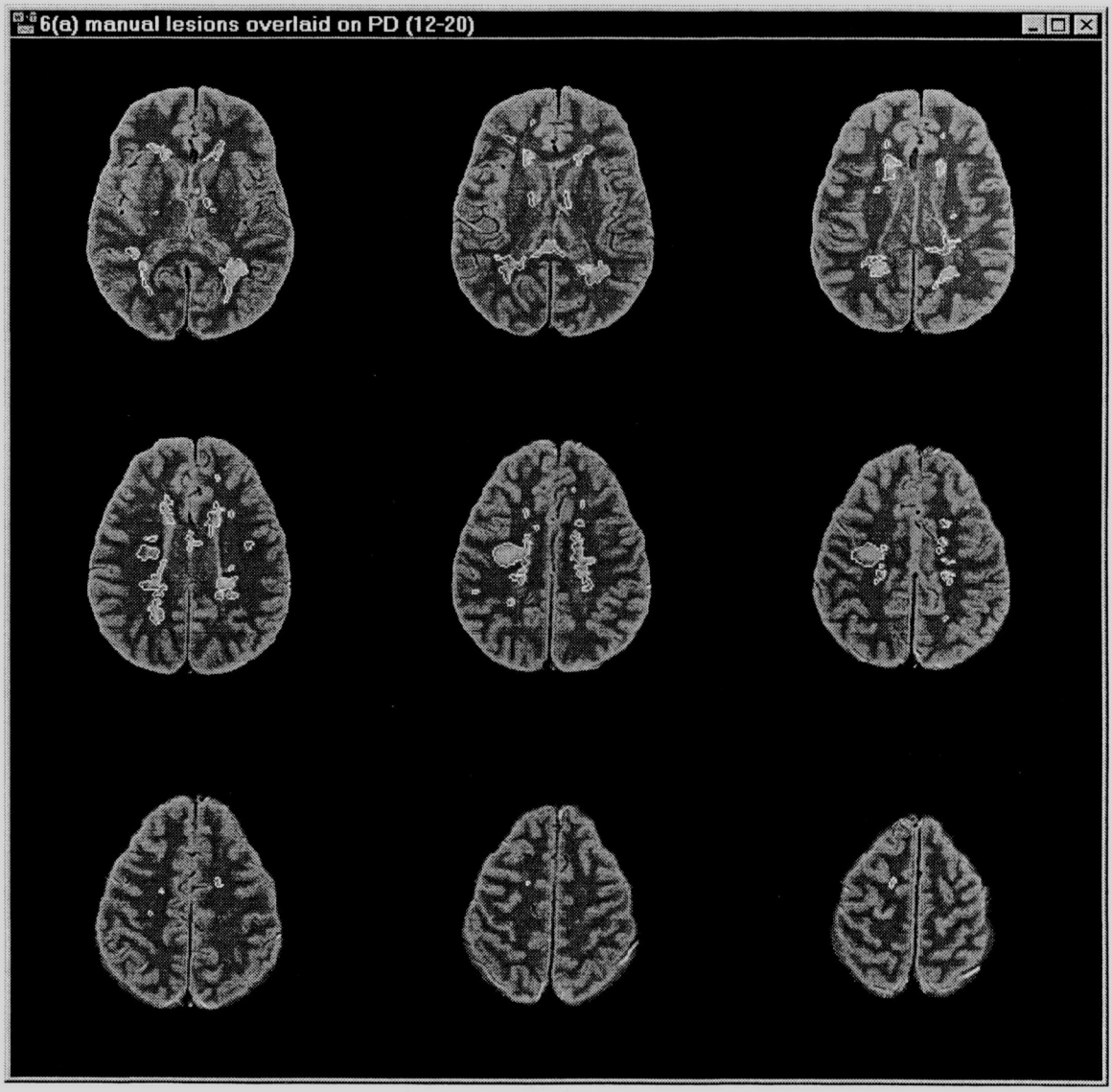

Figure 6: Manual Segmentation results on the central slices (12-20) of the volume

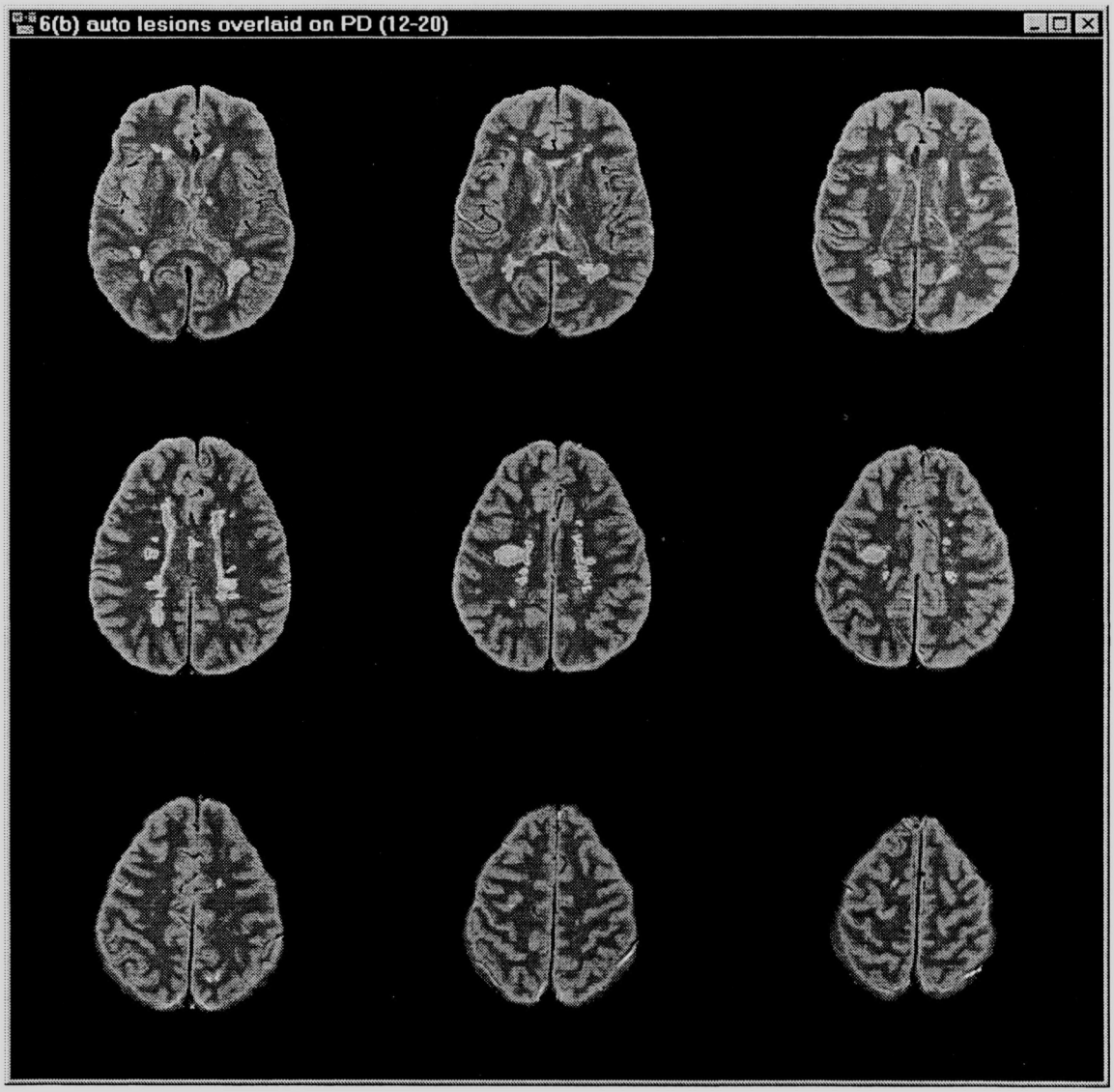

Figure 7: Auto Segmentation results on the central slices (12-20) of the volume

For a quantitative evaluation, we use a similarity index measure defined in [9]. Similarity indices are obtained for the central slices at two different stages of image analysis and shown as a graph in Figure 8. The increasing values of similarity indices for step 2 results over step 1 results show the segmentation improvement.

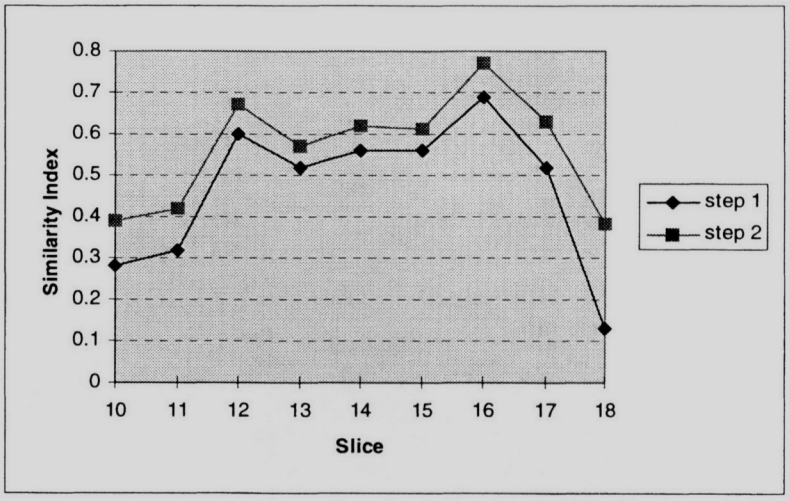

Figure 8: Graph to show how the similarity index improves from step1 to step2.

To evaluate the segmentation performance over the whole volume and over different data sets, we have calculated the total lesion volume for the whole brain using the manual and the automatic segmentation methods for each data set and compare the results using linear regression [10]. Results for each slice of a particular volume are shown in Figure 9.

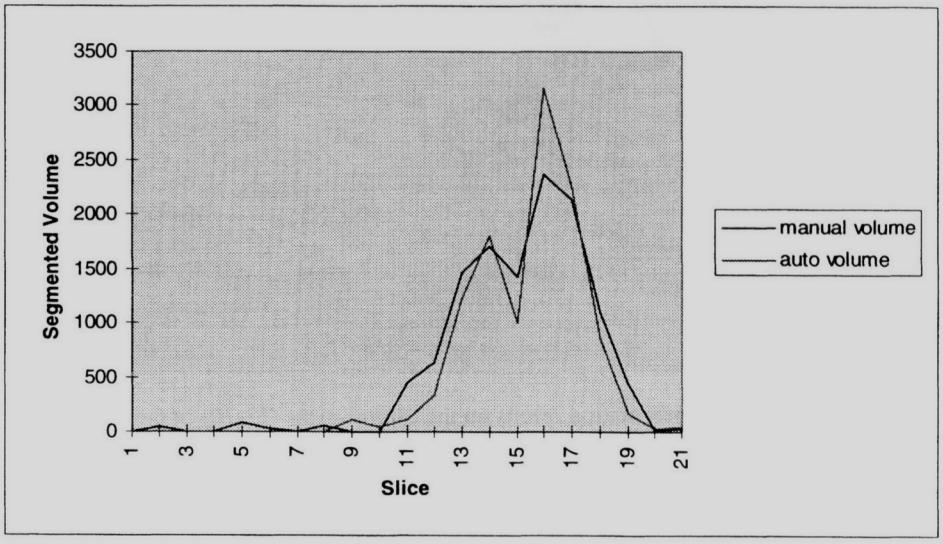

Figure 9: Segmented Volume, manual vs. auto, on all slices of the volume.

Figure 9 shows that there are no false positive lesio ns in the slices below slice 10, and it also shows how well the auto volumes track the manual volumes overall.

Figure 10 shows the correlation between the manually-found lesion volumes and the auto-found lesion volumes for 8 different data sets. For lesion volumes below 2000mm^3, the lesions are underestimated compared with the manual. This is because the data sets with low lesion volumes contain no hot lesions (only subtle lesions) and the performance of the method is not fully satisfactor y in segmenting subtle lesions. Calculations show a correlation figure of 0.972 over the measured range with the manually predicted volume , which compares very well with other published results [10].

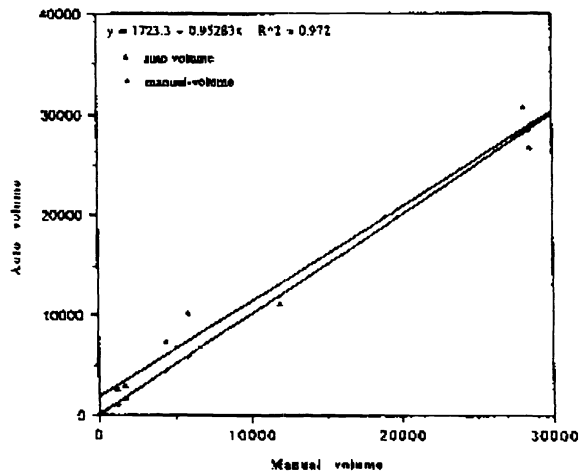

Figure 10: Segmentation performance on 8 different data sets with lesion volumes ranging from 200-28000 mm^3.

4. CONCLUSION

We have proposed a method for the image analysis of MRI data to segment MS-lesions. The method is in its initial stages of development and shows promising directions for characterization and quantit ation of MS-lesions. We have shown how the MRI data can be analyzed and segmented using a ratio filter transformation and multispectral enhancement operations. The method does not require any user-defined regions of interest. We have demonstrated the segmentation performance of the method quantitatively using similarity indices. The method has also shown a reliable and consistent performance on the whole volume for 8 different data sets. Results are evaluated by calculating the similarity indices for the slices with lesions and by calculating the lesion volumes. The similarity figures show values as high as 0.75 with manually outlined lesions and a volume correlation of 0.972. Our future work will include improving the performance of the method by using some spatial information and testing the method on different PD/T2 echo sequences and on time series data.

ACKNOWLEDGMENTS

The authors wish to thank Dr. D. Paty and Dr. D. Li at the University of British Columbia MS/MRI group for their helpful comments and providing the data.

REFERENCES

[1] B. Johnston, M.S. Atkins, "Segmentation of Multiple Sclerosis Lesions in Intensity Corrected Multispectral MRI," *IEEE Transactions on Medical Imaging*, Vol. 15, No. 2, pp. 1-15, 1996.

[2] H. S-Zadeh, J. P. Windham, D. J. Peck, "Optimal Linear Transformation for MRI Feature Extraction," *IEEE Transactions on Medical Imaging*, Vol. 15, No. 6, pp. 749-766, 1996.

[3] J. K. Udupa, L. Wei, S. Samarasekera, Y. Miki, M. A. Van Buchem and R. I. Grossman, " Detection and Quantification of MS Lesions Using Fuzzy Topological Principles," in *SPIE Proceedings* , Vol. 27, 10, pp. 81-87, 1996.

[4] M. Kamber, R. Shinghal, D. L. Collins, G. S. Francis and A. C. Evans, " Model-Based 3-D Segmentation of Multiple Sclerosis Lesions in Magnetic Resonance Brain Images," in *IEEE Transactions on Medical Imaging*, Vol. 14, No. 3, pp. 442-453, 1995.

[5] M. W. Vannier, R. L. Butterfield, D. Jorden, W. A. Murphy, R. G. Levitt and M. Gado, " Multispectral Analysis of Magnetic Resonance Images," *Radiology.*, Vol. 154, pp. 221-224, 1985.

[6] M. S. Atkins and B. Mackiewich, " Automatic Segmentation of the Brain in MRI," *Springer-Verlag Lecture Notes in Computer Science.*, 1131, pp. 210-216, 1996.

[7] W. K. Pratt, " Chapter 12.9. Multispectral Image Enhancement,"*Digital Image Processing*, New York: Wiley, 1978.

[8] H. S-Zadeh, J. P. Windham, D. J. Peck and A. E. Yagle, "A Comparative Analysis of Several Transformations for Enhancement and Segmentation of Magnetic Resonance Image Scene Sequences," *IEEE Transactions on Medical Imaging*, Vol. 11, No. 3, pp. 302-318, 1992.

[9] A. Zijdenbos, B. M. Dawant, R. A. Margolin and A. C. Palmer, "Morphometric Analysis of White Matter Lesions in MR Images: Method and Validation," *IEEE Transactions on Medical Imaging*, Vol. 13, No. 4, pp. 716-724, 1994.

[10] A. Zijdenbos, A. Evans, F. Riahi, J. Sled, J. Chui and V. Kollokian, "Automatic Quantification of Multiple Sclerosis Lesion Volume Using Stereotaxic Space," *Springer-Verlag Lecture Notes in Computer Science.*, 1131, pp. 439-448, 1996.